Hybrid-Integrated 4 × 4 Optical Gate Matrix Switch Using Silica-Based Optical Waveguides and LD Array Chips

Yasufumi Yamada, Hiroshi Terui, Yasuji Ohmori, Makoto Yamada, Akira Himeno, and Morio Kobayashi

Abstract— **Fabrication and characteristics of a hybrid-integrated optical gate matrix switch was studied. The switch was composed of a silica-based single-mode guided-wave circuit, and two InGaAsP gate array chips, each of which comprised eight laser diode optical gates. The gate array chips were assembled on the guided-wave circuit using hybrid integration technique. Insertion loss of the fabricated 4 × 4 matrix switch was scattered among switching paths and ranged from 26 to 33 dB. The switch was applicable to a 400 Mb/s signal system with a bit error rate of 10^{-9}. The numerical analysis has clarified that the residual reflectivity at the LD gate and waveguide facets caused the loss scattering among the paths and reduction of the residual reflectivity is essential for improving the switch characteristics.**

I. Introduction

OPTICAL switches play an important role in advanced optical communication systems and optical signal processing systems. To date, three types of switches have been investigated: a space-division type [1], [2], a time-division type [3], and a wavelength-division type [4]. Among them, space-division type switches are expected to have the widest bandwidth. Research on space-division switches has concentrated so far on optical beam deflection type switches such as an 8 × 8 $LiNbO_3$ switch [1] and a 4 × 4 InGaAsP matrix switch [2]. Another type of space-division switch is an optical gate-type switch featuring point-to-multipoint switching [5]. This function is suitable for optical video signal distribution from a center station to multiple subscribers. Furthermore, it is possible to utilize this type of switch in optical signal processing systems since the optical gates are compatible to optical logic.

The authors have studied fabrication of a guided-wave 4 × 4 optical gate matrix switch, composed of a silica-based guided-wave circuit and laser diode optical gates (LD gates) assembled in hybrid fashion [6], [7]. Research on the switch has mainly focused on circuit design and feasibility study of waveguide fabrication and waveguide-gate coupling. However, the integration process applicable for assembling sixteen optical gates remains to be studied in view of practical use of the switch. Moreover, the characteristics of the hybrid integrated switch, such as bandwidth and influence of reflected light on LD gate performance, require further study.

This paper describes the fabrication and characteristics of the 4 × 4 optical gate matrix switch. First, the fabrication of the switch, especially integration proceduce of the LD gates, is described. Then, switch characteristics and signal transmission are studied experimentally. The effect of reflectivity at the waveguide-gate coupling points is also discussed.

Manuscript received December 22, 1991; revised October 17, 1991.

Y. Yamada, H. Terui, Y. Ohmori, M. Yamada, and M. Kobayashi are with NTT Opto-electronics Laboratories, Tokai-mura, Ibaraki-ken, 319-11, Japan.

A. Himeno is with NTT Communication Switching Laboratories, 3-9-11, Midori-cho, Musashino-shi, Tokyo, 180, Japan.

IEEE Log Number 9105230.

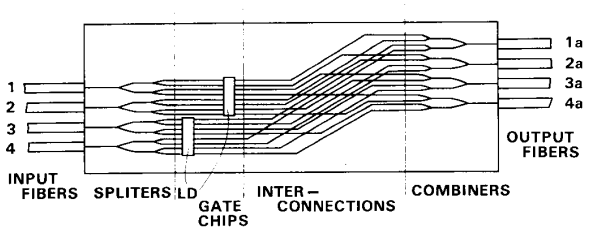

Fig. 1. Schematic illustration of a 4 × 4 optical gate matrix switch.

II. Fabrication of 4 × 4 Optical Gate Matrix Switch

A. Switch Configuration

A schematic illustration of a hybrid integration type 4 × 4 optical gate matrix switch is shown in Fig. 1. Two LD gate array chips, each with eight LD gates, are assembled with the silica-based guided-wave circuit. The switch dimension is 5 mm × 40 mm. Ordinary single-mode fibers (not polarization maintaining fibers) are butt-coupled at the ends of the waveguides.

Optical switching is based on stimulated light amplification and absorption in a laser diode [8]. When an appropriate current is injected into the LD gate, the gate acts as an optical amplifier and the on-state is obtained. One-to-one connection is performed by opening one of the sixteen gates. If multiple gates are opened at the same time, one-to-multipoint connection can be made.

B. Guided-Wave Circuit

The guided-wave circuit was made of single-mode silica-based ridge type channel waveguides on an Si substrate. A cross-sectional view of the channel waveguide is shown in Fig. 2. The SiO_2–TiO_2 core was 5 μm wide and 5 μm deep,

0733–8724/92$03.00 © 1992 IEEE

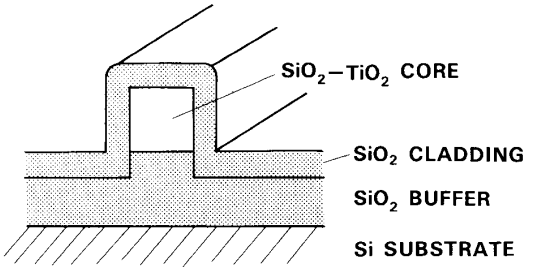

Fig. 2. Cross-sectional view of silica-based ridge waveguide.

and the SiO_2 cladding was 3 μm thick. The core-cladding refractive-index difference was 0.7%.

The circuit was composed of splitters, LD gate chip insertion grooves, interconnections, and combiners. Each splitter circuit was constructed tandem connection of two branching circuits to split input optical power uniformly. The LD gate chip insertion groove was 320 μm wide. The interconnection circuits were made of intersecting and reflection-bending waveguides to make the circuits compact [9]. The bending and the intersecting patterns were designed so that the intersecting points do not concentrate at the same points. The combiner circuits were formed in an inverse configuration of the splitter circuit.

In order to obtain the guided-wave circuit insertion loss, the guided-wave circuit was cut into two parts; the splitter side circuit including the splitters and the combiner side circuit including the interconnections and the combiners. The average losses among 16 paths for the splitter side and the combiner side circuits were 9 dB with the input fiber coupling loss and 16 dB with the output fiber coupling loss, respectively. The average total circuit insertion loss was, then, estimated to be 25 dB.

C. Laser Diode Optical Gate Chip

The LD gate chip included eight BH-type InGaAsP laser diodes with SiO anti-reflection coating (AR coating) on both facets [10]. The laser diodes were spaced 200 μm each other. In order to make LD gate integration easy, the gate chip width was chosen 300 μm, smaller than the insertion groove width. The residual reflectivity of each facet with AR coating was estimated to be less than 0.1%. Peak wavelength of spontaneous emission, which was 1.32 μm before AR coating, shifted to 1.30 μm after AR coating.

D. LD Gate Chip Assembly

Prior to LD gate chip assembly, loss increment due to gate displacement was examined using an experimental set-up shown in Fig. 3(a). Output power versus gate lateral displacement at 80-mA gate current is shown in Fig. 3(b). Vertical displacement resulted in almost the same output power change. For 2-dB loss increment, displacement tolerance was ± 1 μm.

In order to achieve highly accurate optical LD gate chip alignment, each LD gate chip was integrated in the insertion groove in an up-side down fashion as shown in Fig. 4. The

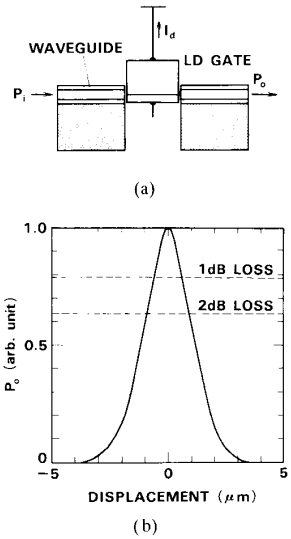

Fig. 3. Relation between LD gate insertion loss and lateral displacement.

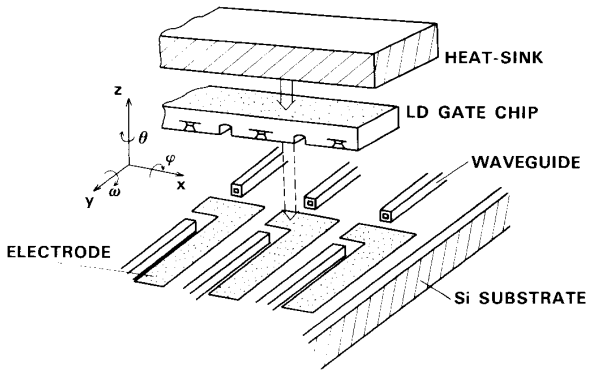

Fig. 4. Schematic diagram of hybrid integration process of the LD gate chip.

height of the waveguide core centers from the electrodes was chosen equal to that of the active layers of the optical gate chips when the LD gate chip was inserted in up-side down fashion. Therefore, alignment in the z direction was accomplished only by placing the optical gate chip on the electrode surface. Angular alignments around x axis (φ) and y axis (ω) could also be performed automatically.

Alignment in the y direction was performed by microscope observation. Lateral alignment in the x direction and angular alignment around z axis (θ) were carried out using optical gates as photodetectors [11], as shown in Fig. 5. Waveguides on both the left and right sides of the optical gate array were exited by 1.3-μm LD light sources. Alignment was performed by monitoring the detected photo-current from the gates.

Photo-current change during the alignment process is shown in Fig. 5(a) and (b). When the angular misalignment exists with respect to θ, the peak positions for two gates G2 and G7 were different from each other (Fig. 5(a)). The angle θ was adjusted so that the two peaks were coincident as shown in Fig. 5(b). After setting the optical gate at the peak position, the optical gate chip was fixed on the Au-Sn electrode by heating.

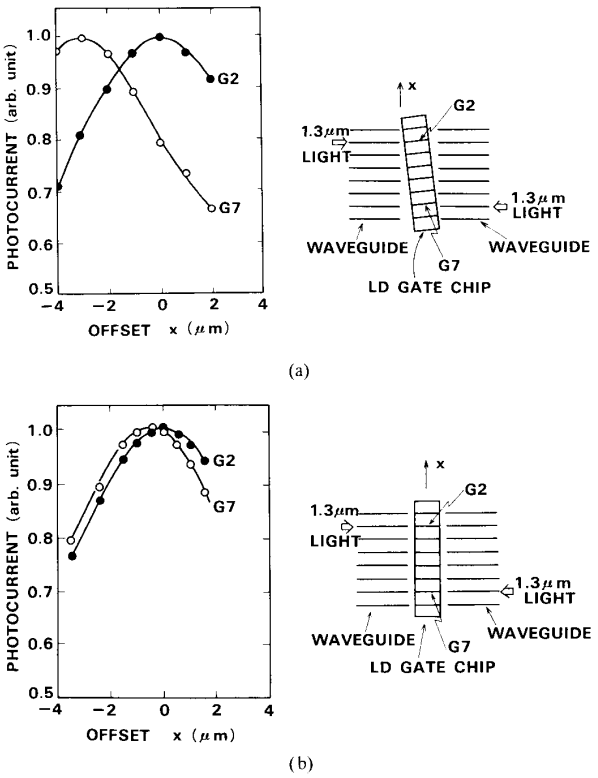

Fig. 5. Photo-current change during alignment. a) Before angular alignment for θ. b) After angular alignment for θ.

Fig. 6 shows an example of the output spontaneous emission power at 80-mA injection current from the integrated optical gate array detected through fibers coupled to output ports of the circuit. The spontaneous emission power was −29−−30 dBm. On the other hand, the spontaneous emission power without misalignment between the gate and the waveguide was estimated to be −12 dBm through the same experimental setup as Fig. 3(a). Since the typical loss for the combiner side circuit was −16 dB, the spontaneous emission power from the output fiber of the guided-wave circuit is calculated to be −28 dBm if there is no misalignment. The loss increase after the hybrid integration is, then, estimated to be 1–2 dB. This value corresponds to the alignment accuracy of ±1 μm.

E. Optical Fiber Connection

Fiber-waveguide connection was carried out using the optical gate as a photodetector. A 1.3-μm light was launched into the switch circuit from the fiber, and the fiber was aligned so as to obtain the maximum photo-current. After the fiber-waveguide alignment was completed, the fibers were fixed by UV curable cement.

III. 4 × 4 Optical Gate Matrix Switch Characteristics

A. Static Characteristics

A 1.30-μm laser diode was used as a signal source. Signal light was launched into an input fiber of the switch and output

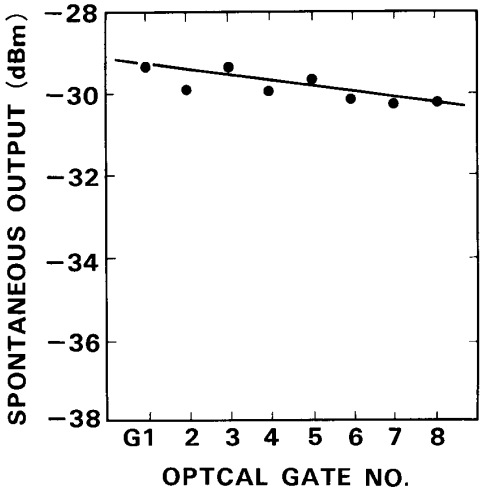

Fig. 6. Output spontaneous emission power detected at waveguide output ports.

signal from an output fiber was detected by an optical power meter. Since the connected optical fibers were not polarization maintaining fibers, the measurements were carried out under nonpolarization conditions.

Fig. 7 shows the measured insertion loss for some paths of the switch. They are paths 3-2a (input fiber 3-gate G10-output fiber 2a), 3-3a (input fiber 3-gate G11-output fiber 3a) and 4-1a (input fiber 4-gate G13-output fiber 1a). The gates G10, G11 and G13 were in the same chip. When the injection current was less than 80 mA, loss decreased monotonically with the injection current. At the 80-mA injection current, insertion loss was 26 dB for path 3-2a, 29 dB for path 3-3a and 32 dB for path 4-1a. When the injection current exceeded 80 mA, insertion loss became unstable and loss scattering among paths increased remarkably. Lasing of the gates also often took place.

Table I lists the measured static characteristics of the fabricated switch. The optical gates were driven at 80-mA injection current. Insertion loss ranged from 26 to 33 dB among the paths. Since the average guided-wave circuit loss was estimated 25 dB as mentioned in Section II-B, gate insertion loss was estimated to be 1–8 dB. The extinction ratio, defined as the ratio of the output signal at 80 mA and at 0 mA, was 25–30 dB. Crosstalk was 15–22 dB and the spontaneous emission was −29−−30 dBm.

The main origin of the loss scattering from path to path seems to be due to the effect of reflection from the LD gate facets and the waveguides facets, not to misalignment between the gates and waveguides. This is because the spontaneous emission deviation among gates was about 1 dB at a 80-mA injection current as shown in Fig. 6, and the alignment accuracy was estimated to be within ±1 μm. If the origin of the loss scattering among paths was in misalignment, the spontaneous emission deviation should have been much more than 1 dB. The effect of the residual reflection due to imperfect antireflection coating will be discussed later.

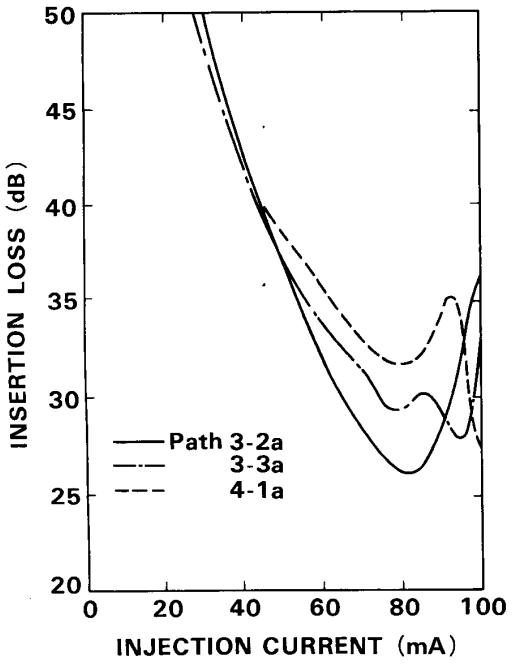

Fig. 7. Injection current dependence of insertion loss for paths 3-2a, 3-3a, and 4-1a.

TABLE I
STATIC CHARACTERISTICS OF FABRICATED 4 × 4 OPTICAL GATE SWITCH

TOTAL INSERTION LOSS	26–33 dB (I = 80 mA)
OPTICAL CIRCUIT LOSS	25 dB
LD GATE INSERTION LOSS	1–8 dB
SPONTANEOUS EMISSION POWER	−30 dBm (I = 80 mA)
EXTINCTION RATIO	25–30 dB
CROSSTALK	15–22 dB

Static characteristics were also evaluated at 1.29- and 1.31-μm wavelength. The measured characteristics were almost the same as those at 1.30 μm. Therefore, this switch is usable in a 1.29–1.31-μm wavelength range. This indicates that the switch is applicable to a bi-directional wavelength multiplexed system [12].

B. Signal Transmission Experiment

The possible signal bit rate transmitting through the switch is determined from the received optical power and power penalty to compensate the degradation of the signal-to-noise ratio. In the case of the LD-gate switch, the power penalty is mainly due to the spontaneous emission noise [12], [13]. In order to estimate the possible signal rate, the received optical power and power penalty were obtained experimentally.

The bit-error-rate measurements were performed for three cases: A) the signal light was launched into the fabricated switch and the output signal was detected by an InGaAs avalanche photodiode (APD), B) the signal was launched into the switch and the output signal filtered through a 5-nm-wide optical bandpass filter was detected by APD, C) the signal was directly detected by APD.

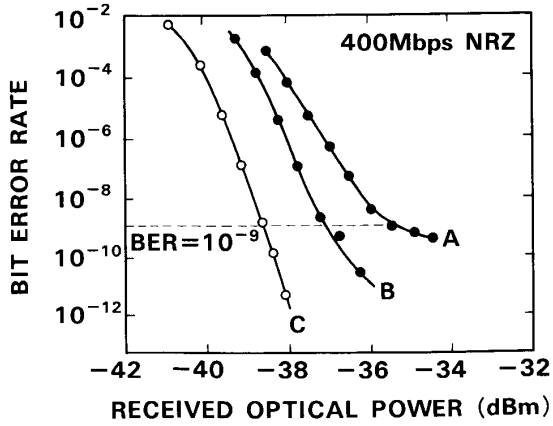

Fig. 8. Bit error measurement results: line A: with spontaneous emission of −30 dBm, line B: with spontaneous emission of −39 dBm, line C: without spontaneous emission.

Fig. 8 shows the relationship between the received optical power and the bit error rate (BER) measured for a 400-Mb/s NRZ signal. Line A is the result for the case A. The detectable optical power necessary for obtaining BER of 10^{-9} was −35.5 dBm. Here, a spontaneous emission noise was −30 dBm. Line B is the result for the case B. The optical detectable power necessary for BER of 10^{-9} was reduced to −37 dBm, because the spontaneous emission noise was reduced to −39 dBm. In case C, the detectable power for BER of 10^{-9} was −38.5 dBm (Line C). This corresponds to the detectable power without spontaneous emission noise. Comparing Lines A and C, the power penalty due to −30 dBm spontaneous emission noise was estimated to be 3.0 dB.

Accordingly, it is clear that the switch is applicable to 400 Mb/s signal transmission if the input signal level is more than −2.5 dBm. This is because insertion loss of the fabricated switch was at most 33 dB as shown in Table I, and therefore, the output power from the switch is expected to be more than −35.5 dBm.

The 4 × 4 matrix switches were applied to a space-division optical switching system and 400 Mb/s video signal exchange experiments were performed successfully [15].

IV. EFFECT OF RESIDUAL REFLECTIVITY

As mentioned in Section III, fairly large insertion loss scattering among paths was observed in the fabricated switch. In this section, origin of the loss scattering and conditions for improving switch characteristics are discussed.

A. Numerical Analysis for Integrated LD Gate Behavior

Fig. 9(a) shows the schematic diagram of the integrated LD gate. When reflectivities at the LD gate facet R_L and/or the waveguide facet R_{g0} are not zero, air-gaps between the facets form external cavities for the LD gate. In this figure, d_1 and d_2 are the length of the left- and right-side cavity, respectively. η_i is the waveguide to LD gate coupling efficiency with distance d_i $(i = 1, 2)$, and ζ_i is the coupling efficiency of

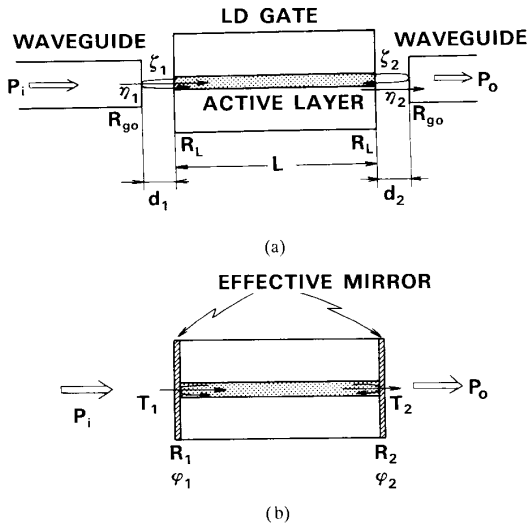

Fig. 9. External cavity model for the integrated LD gate.

reflected light to LD gate, that is, the coupling efficiency of the LD gate output light reflected to the gate by a mirror with 100% reflectivity at distance d_i $(i = 1, 2)$. Here, suffix $i = 1$ and 2 indicate the left-side and the right-side external cavities, respectively. Considering the coupling efficiency ζ_i, the practical remaining reflectivity at the waveguide facet R_{gi} is obtained as

$$R_{gi} = R_{g0}\zeta_i \quad (i = 1, 2). \tag{1}$$

The LD gate with external cavities in Fig. 9(a) can be considered as the LD gate having effective mirrors with complex amplitude reflection coefficient at both facets as shown in Fig. 9(b) [14]. The complex amplitude coefficient r_i is expressed as

$$r_i = \sqrt{R_i}\exp(-\varphi_i) \quad (i = 1, 2). \tag{2}$$

Here, R_i and φ_i are the reflectivity and the phase shift at the effective mirror. R_i is expressed as

$$R_i = \frac{R_L - 2\sqrt{R_L R_{gi}}\cos\delta_i + R_{gi}}{1 - 2\sqrt{R_L R_{gi}}\cos\delta_i + R_L R_{gi}} \simeq R_L - 2\sqrt{R_L R_{gi}}\cos\delta_i + R_{gi} \quad (i = 1, 2). \tag{3}$$

with

$$\delta_i = (2\pi/\lambda)2\mathrm{n}d_i \quad (i = 1, 2). \tag{4}$$

Here, R_L and R_{g0} are assumed to be small compared to unity. A transmittance T_i of the effective mirror is also written as

$$T_i = \frac{\eta_i(1 - R_L)(1 - R_{gi})}{1 - 2\sqrt{R_L R_{gi}}\cos\delta_i + R_L R_{gi}} \varphi\eta_i \simeq \quad (i = 1, 2). \tag{5}$$

In (3)–(5), δ_i is phase difference for round trip in the external cavity, n is the refractive index of the external cavity and $n = 1$ in this case, and λ is the wavelength of signal light.

In the following calculation, the parameter values are assumed as follows, corresponding to the fabricated switch parameters: The cavity lengths are $d_1 = 10 + x$ μm and $d_2 = 10 - x$ μm $(x < 1)$. The waveguide spot radius is 3 μm, and the LD gate spot radius is 1.2 μm horizontally and 0.8 μm vertically. Coupling efficiencies for the right-side and the left-side cavities are equal each other, that is, $\eta_i = \eta_i = \eta$ and $\zeta_1 = \zeta_2 = \zeta$, because $d_1 \simeq d_2$, and from those spot radius values, M and ζ are both estimated to be 7 dB based on the near-field overlap integral with the LD-gate and waveguide. The residual reflectivity at LD gate facets R_L is 0.1%. The reflectivity at waveguide facet R_{g0} is 3%.

Applying the gain equation for the optical amplifier [13], gate gain G can be obtained as

$$G = T_{\mathrm{eff}}^2 G_0/(1 - 2R_{\mathrm{eff}}G_0\cos\Omega + R_{\mathrm{eff}}^2 G_0^2). \tag{6}$$

with

$$R_{\mathrm{eff}} = \sqrt{R_1 R_2}. \tag{7}$$

and

$$T_{\mathrm{eff}} = \sqrt{T_1 T_2}. \tag{8}$$

where R_{eff} and T_{eff} are the effective reflectivity and transmittance of the integrated LD gate facet, and G_0 is the single pass gain of the LD gates. Ω is the phase difference of signal light in the LD gate with the external cavities and is expressed as

$$\Omega = (2\pi/\lambda)2n_L L + \varphi_1 + \varphi_2. \tag{9}$$

where n_L is the modal refractive index of the LD gate and L is the LD gate length.

The external cavity length dependence of the effective reflectivity R_{eff} is calculated using (3) and (7). The relationship between R_{eff} and x is shown in Fig. 10. It is found that the effective reflectivity R_{eff} is very sensitive to external cavity length change x. Even if the cavity lengths change by 0.3 μm, the reflectivity changes from its maximum ($R_{\mathrm{eff}} = 1.15\%$) to a minimum ($R_{\mathrm{eff}} = 0.25\%$).

LD gate behavior for $R_{\mathrm{eff}} = 1.15\%$ and $R_{\mathrm{eff}} = 0.25\%$ was, then, calculated using (6). The single pass gain G_0 of the LD gate was assumed to be 20 dB. The relationship between the LD gate gain G and the signal light phase difference Ω is shown in Fig. 11. The gain-ripples are observed for the cases of $R_{\mathrm{eff}} = 1.15\%$ and 0.25%. However, the magnitude of the ripples are quite different from each other. For $R_{\mathrm{eff}} = 1.15\%$, the maximum gain $G_{\max}$ and the minimum gain $G_{\min}$ are 30 and -1 dB, respectively. The magnitude of gain-ripple ΔG is, then, estimated to be 31 dB. For $R_{\mathrm{eff}} = 0.25\%$, on the other hand, $G_{\max}$ is 8 dB and $G_{\min}$ is 4 dB. ΔG is reduced to 4 dB.

Accordingly, the influence of the residual reflectivity on integrated the LD gate behavior is clarified. When the residual reflectivity exists, the integrated LD gate behavior is influenced by the external cavity length. In case of the fabricated 4 × 4 switch, the external cavity length was determined within an accuracy of ± 1 μm. However, the effective reflectivity can be changed from its maximum to its minimum if the external cavity changes only 0.3 μm as shown in Fig. 10. Therefore, this will result in the scattering of the LD gate switch insertion loss among paths.

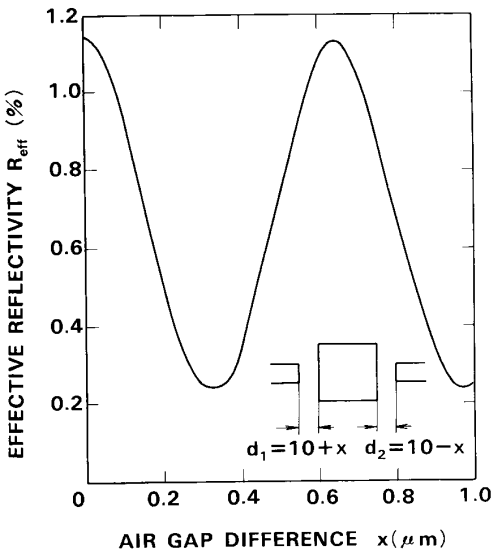

Fig. 10. Relation between the effective reflectivity R_{eff} of integrated LD gate and the external cavity length change x.

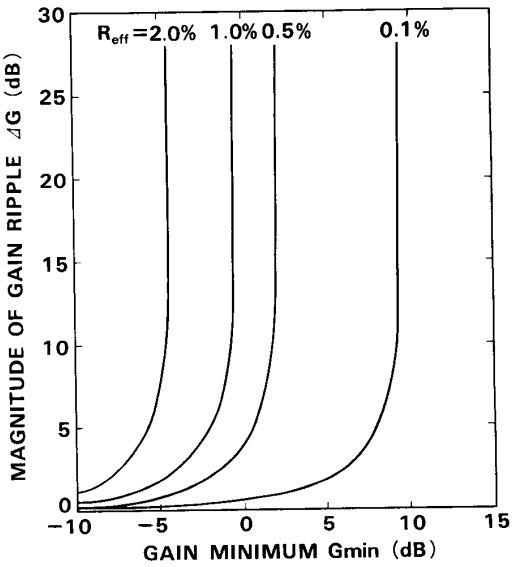

Fig. 12. Relation between the gain minimum G_{min} and the gain ripple ΔG, with effective reflectivity R_{eff} as a parameter.

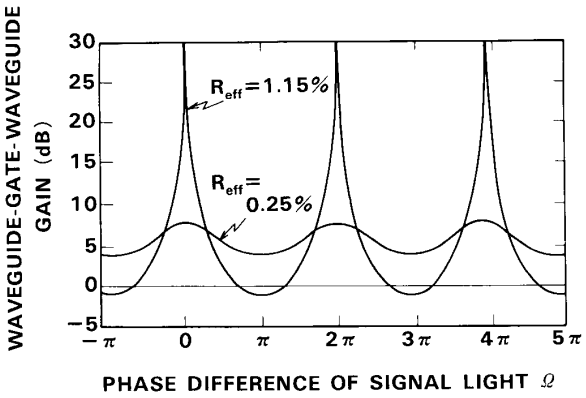

Fig. 11. Gain-ripple of the LD gate for R_{eff} = 1.15% and 0.25%.

B. Anti-Reflection Coating Condition

In order to improve the hybrid integration type 4×4 optical switch, reduction of the residual reflectivity at the waveguide and LD gate facets is essential. Therefore, antireflection coating conditions are studied.

From (6), the maximum and the minimum gains G_{max} and G_{min} are expressed as

$$G_{max} = T_{eff}^2 G_0/(1 - R_{eff}G_0)^2. \quad (10)$$

$$G_{min} = T_{eff}^2 G_0/(1 + R_{eff}G_0)^2. \quad (11)$$

and the magnitude of gain-ripple ΔG is

$$\Delta G = G_{max}/G_{min} = (1 + R_{eff}G_0)^2/(1 - R_{eff}G_0)^2. \quad (12)$$

In order to clarify the required value of effective reflectivity R_{eff}, the relationship between G_{min} and ΔG is calculated using (10) and (12) with R_{eff} as a parameter. The results are shown in Fig. 12. If R_{eff} is large, gain-ripple ΔG increased remarkably even when gain minimum G_{min} is small. From a practical point of view, the gain-ripple of the LD gate should be small to eliminate instability. Therefore, R_{eff} gives the limit of the attainable gain of the integrated LD gate. When the permissive gain-ripple is assumed to be 3 dB, for example, the attainable G_{min} values are -7 dB for R_{eff} = 2.0% and 7 dB for R_{eff} = 0.1%. In order to use the LD gate as an optical amplifier ($G_{min} > 0$ dB), R_{eff} must be less than 0.5%.

Next, the required AR coating condition of the waveguide and the LD gate facets for operating the LD gate as an amplifier is studied. As shown in Fig. 10, the effective reflectivity R_{eff} changes with the external cavity length. Therefore, the AR-coating condition is examined using the maximum value of reflectivity, R_{eff}^{max}.

R_{eff}^{max} is estimated through (3) and (7) as,

$$R_{eff}^{max} = \sqrt{R_1^{(max)} R_2^{(max)}} = \left(\sqrt{R_L} + \sqrt{\zeta R_{g0}}\right)^2. \quad (13)$$

Fig. 13 shows the calculated result for (13). Since R_{eff}^{max} should be less than 0.5% in order to operate the LD gate as the amplifier, the residual reflectivity of the waveguide facet R_{g0} should be reduced to less than 2%. When R_{eff}^{max} is reduced to be less than 0.5%, the insertion loss of the 4×4 optical gate switch will be less than 25 dB for every path. If R_{g0} and R_L can be decreased to less than 0.2 and 0.02%, respectively, R_{eff}^{max} will be less than 0.1%, and the LD gate will have more

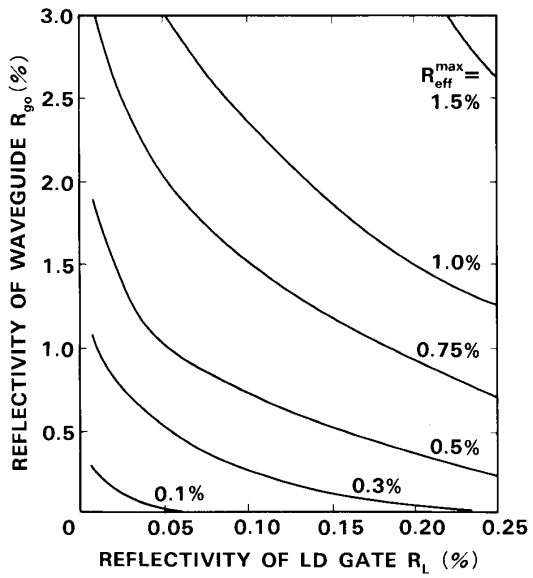

Fig. 13. Relation among the reflectivity R_l of LD gate, reflectivity R_{g0} of waveguide facets and the maximum effective reflectivity $R_{\text{eff}}^{\max}$.

than 5-dB gain; insertion loss of the switch will, then, be reduced to less than 20 dB for all paths when the waveguide circuit loss is 25 dB.

Through the discussion, it is clarified that the antireflection coating both at the LD gate and the waveguide facets is the key to improving switch characteristics. By reducing the residual reflectivity, the insertion loss as well as the loss scattering among paths will be decreased.

V. Conclusion

Fabrication and characteristics of a hybrid integration type 4 × 4 optical gate matrix switch were described. The switch was composed of a silica-based guided-wave switch circuit and 16 laser diode gates.

In order to integrate 16 optical gates, two LD gate chips, each with eight laser diode gates, were used. They were integrated on a guided-wave circuit surface in an up-side down fashion. This made it possible to achieve not only vertical direction alignment but also angular alignments around two axes only by placing the gate chips on the waveguide. The lateral alignment was performed through monitoring the photocurrent detected by the optical gate acting as a photodiode.

The insertion loss of the fabricated 4 × 4 optical switch at 80 mA injection current was 26–33 dB. The spontaneous emission was about −30 dBm. The bit error rate measurements indicated that the detectable power necessary for transmitting the 400 MB/s signal with BER of 10^{-9} was −35.5 dBm including the power penalty for compensating the spontaneous emission noise. This switch is, therefore, applicable to 400 Mb/s signal switching system when the input signal is more than −2.5 dBm.

The numerical analysis based on the external cavity laser model revealed that the waveguide and the LD gate facets formed the external cavities of the integrated LD gate. This results in the insertion loss scattering among the switch paths. The improved optical switch can be achieved by eliminating the residual reflectivity both at the LD gate and waveguide facets.

Acknowledgment

The authors wish to thank N. Takato and M. Yasu for their experimental helps.

References

[1] P. Granestrand, "Strictly nonblocking 8 × 8 integrated optical switch matrix," *Electron. Lett.*, vol. 22, pp. 816–818, 1986.
[2] S. Sakano, H. Inoue, H. Nakamura, T. Katsuyama, and H. Matsumura, "InGaAsP/InP monolithic integrated circuit with lasers and an optical switch," *Electron. Lett.*, vol. 22, pp. 594–596, 1986.
[3] M. Sakaguchi and H. Goto, "High speed optical time-devision and space-devision switching," *IOOC/ECOC' 85. Tech. Dig.* (Venezia) vol. 2, 1985, pp. 81–88.
[4] T. Yasui and H. Goto, "Overview of optical switching technologies," *IEEE Commun. Maga.*, vol. 25, 1987, pp. 10–15.
[5] A. Himeno and M. Kobayashi, "4 × 4 optical gate matrix switch," *J. Lightwave Technol.*, vol. LT-3, pp. 230–235, 1985.
[6] A. Himeno, H. Terui, and M. Kobayashi, "Guided-wave optical gate matrix switch," *J. Lightwave Technol.*, vol. 6, pp. 30–35, 1988.
[7] H. Terui, A. Himeno, Y. Yamada, and M. Kobayashi, "Single-mode guided-wave optical gate matrix switch," in *Tech. Dig. ECOC' 87.*
[8] M. Ikeda, "Laser diode switch," *Electron. Lett.*, vol. 17, pp. 899–900, 1981.
[9] A. Himeno, M. Kobayashi, and H. Terui, "High-silica single-mode optical reflection bending and intersecting waveguides," *Electron. Lett.*, vol. 21, pp. 1021–1022, 1985.
[10] M. Ikeda, "Signal-monitoring characteristics for laser-diode optical switches," *J. Lightwave Technol.*, vol. LT-3, pp. 909–913, 1985.
[11] T. Mukai, Y. Yamamoto, and T. Kimura, "S/N and error rate performance in AlGaAs semiconductor laser preamplifier and linear repeater systems," *IEEE J. Quantum. Electron.*, vol. QE-18, pp. 1560–1568, 1982.
[12] M. Matsunaga, K. Kikuchi, and M. Ikeda, "Optical space division switching system usibg laser diode optical switches," in *Tech. Dig. International Switching Symp.*, pp. 1004–1008, 1987.
[13] J. C. Simon, "GaInAsP semiconductor laser amplifiers for single-mode fiber communications," *J. Lightwave Technol.*, vol. LT-5, pp. 1286–1295, 1987.
[14] L. A. Coldren and T. L. Koch, "External-cavity laser design," *J. Lightwave Technol.*, pp. 1045–4051, vol. LT-2, 1984.
[15] A. Himeno, M. Yamaguchi, Y. Yamada, and T. Matsunaga, "Experimental optical switching system using space-division matrix switches gated by laser diodes," in *Proc. Global Telecommun. Conf.*, 1988.

Yasufumi Yamada was born in Tokyo, Japan, in 1956. He received the B.S., M.S., and Ph.D. degrees from Waseda University in 1980, 1982, and 1990, respectively.

In 1982 he joined NTT Electrical Communication Laboratories, where he has been engaged in research on silica planar lightwave circuits.

Dr. Yamada is a member of the Institute of Electronics, Information and Communication Engineers of Japan, and the Japan Society of Applied Physics.

Hiroshi Terui was born in Aomori, Japan, in 1950. He received the B.S. and M.S. degrees in physics from Tohoku University in 1972 and 1974, respectively.

In 1974, he joined NTT Electrical Communication Laboratories, where he was engaged in research on materials for magnetooptics recording. Since 1976, he has been engaged in research on optical guided-wave devices.

Mr. Terui is a member of the Institute of Electronics, Information and Communication Engineers of Japan and the Japan Society of Applied Physics.

Yasuji Ohmori (M'90) was born in Siga, Japan, on October 20, 1949. He received the B.S. degree in physics from Tohoku University, Japan, in 1974 and the M.S. degree in physics from Tokyo University, Japan, in 1976. He received the Ph.D. degree in electronics engineering from Tokyo University, Japan, in 1985. In 1976 he joined NTT Ibaraki Electrical Communication Laboratory, Ibaraki-ken, Japan, where he was engaged in research on optical fibers. He is now engaging in research on silica planer waveguide circuits.

Dr. Ohmori is a member of the Japan Society of Applied Physics.

Makoto Yamada was born in Niigata, Japan, on September 1, 1960. He received the B.S. and M.S. degrees in electrical engineering from the Technological University of Nagaoka, Niigata, Japan, in 1983 and 1985, respectively. In 1985, he joined NTT Opto-electronics Laboratories, where he was engaged in research on guided-wave optical devices. Since 1989, he has been engaged in research on optical fiber amplifier.

Mr. Yamada is a member of the Institute of Electronics, Information and Communication Engineers of Japan and the Japan Society of Applied Physics.

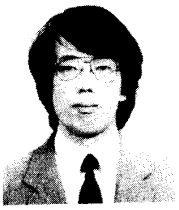

Akira Himeno was born in Miyagi, Japan, on June 20, 1954. He received the B.S., M.S., and Ph.D. degrees from Tohoku University, Japan, in 1977, 1979, and 1991, respectively.

In 1979 he joined NTT Electrical Communication Laboratories, where he was engaged in reserarch on switching systems. From 1983 to 1987 he was involved in the design and fabrication of optical switches. Since 1987 he has been engaged in research on photonic switching systems at NTT Communication Switching Laboratories.

Dr. Himeno is a member of the Institute of Electronics, Information and Communication Engineers of Japan, Japan Society of Applied Physics, and the Optical Society of America.

Morio Kobayashi was born in Nagano, Japan, in 1943. He received the B.S. degree in applied physics from the Science University of Tokyo, in 1967, the M.S. degree in applied physics from Osaka City University, in 1969, and the Ph.D. degree from Osaka Unviersity in 1986.

In 1969, he joined NTT Electrical Communications Laboratories, where he was engaged in research on electrophotography. Since 1975, he has been engaged in research on guided-wave optical devices.

Dr. Kobayashi is a member of the Institute of Electronics, Information and Communication Engineers of Japan and the Japan Society of Applied Physics.